Progress In Electromagnetics Research, Vol. 157, 1–20, 2016

Scattering and Transmission of Waves in Multiple Random Rough Surfaces: Energy Conservation Studies with the Second Order Small Perturbation Method

Tianlin Wang[1], Leung Tsang[1], Joel T. Johnson[2], and Shurun Tan[1, *]

Abstract—Energy conservation is an important consideration in wave scattering and transmission from random rough surfaces and is particularly important in passive microwave remote sensing. In this paper, we study energy conservation in scattering from layered random rough surfaces using the second order small perturbation method (SPM2). SPM2 includes both first order incoherent scattering and a second order correction to the coherent fields. They are combined to compute the total reflected and transmitted powers, as a sum of integrations over wavenumber k_x, in which each integration includes the surface power spectra of a rough interface weighted by an emission kernel function (assuming the roughness of each interface is uncorrelated). We calculate the corresponding kernel functions which are the power spectral densities for one-dimensional (1D) surfaces in 2D scattering problems and examine numerical results for the cases of 2 rough interfaces and 51 rough interfaces. Because it is known that the SPM when evaluated to second order conserves energy, and it can be applied to second order for arbitrary surface power spectra, energy conservation can be shown to be satisfied for each value of k_x in the kernel functions. The numerical examples show that energy conservation is obeyed for any dielectric contrast, any layer configuration and interface, and arbitrary roughness spectra. The values of reflected or transmitted powers predicted, however, are accurate only to second order in small surface roughness.

1. INTRODUCTION

Electromagnetic scattering from layered media with random rough interfaces is of interest due to its wide application to many problems, such as microwave remote sensing [1, 2], nanophotonics and plasmonics [3–5], and layered metamaterials. Methods for determining the fields scattered in these problems can be categorized into analytic methods, numerical methods, and empirical methods.

Classical analytic methods include the small perturbation method (SPM) and the Kirchhoff approximation (KA), which have been extensively studied in [1, 2]. The SPM is a low frequency approach valid for small roughness; most SPM studies consider only the first order terms [6, 7]. High order corrections are included in [8–14], where fourth and higher order corrections are discussed in [11]. The SPM has also been extended to multilayer structures with an arbitrary number of layers [15–18], and the fourth order SPM has been applied to a two-layer geometry in [19]. The KA is a high-frequency approach valid for large curvature roughness, and has been extended to two-layer structure in [20, 21].

To extend the validity region, numerical methods including the Method of Moments (MoM), 3D Numerical Method of Maxwell's equations (NMM3D) [22], Advanced Integral Equation Method (AIEM) [23, 24], and Extended Boundary Condition Method (EBCM) [25–28], etc. have been developed. However, the numerical methods have much higher computational cost than analytic methods, and face

Received 8 August 2016, Accepted 14 September 2016, Scheduled 27 October 2016
* Corresponding author: Shurun Tan (srtan@umich.edu).
[1] Radiation Laboratory, Department of Electrical Engineering and Computer Science, The University of Michigan, Ann Arbor, 48109-2122 MI, USA. [2] ElectroScience Laboratory, Department of Electrical and Computer Engineering, The Ohio State University, Columbus, 43212 OH, USA.

challenges with discretization errors. Numerical methods may not be suitable for layered media with a large number of low contrast interfaces.

Interest has recently been increasing in predicting thermal emissions from layered media with rough interfaces that represent ice sheets [29–31]. In particular, the Ultra-Wideband Software-Defined Microwave Radiometer (UWBRAD) instrument is being developed to observe ice sheet emissions over 0.5–2 GHz, where understanding of the influence of layered roughness on UWBRAD measurements is important. While the interfaces within an ice sheet typically have very small dielectric contrasts, the accumulated effects of hundreds or thousands of interfaces can become significant.

In any simulation of thermal emission from a medium, ensuring energy conservation in the model predictions is crucial. Should energy be not conserved, the brightness temperature computed from the reflected and transmitted powers (in the case of lossless media) would differ, bringing ambiguities in brightness temperature predictions. Requiring energy conservation makes the use of numerical methods more challenging, as roundoff or discretization errors accumulate over a large number of interfaces. Due to the low frequencies of interest for UWBRAD, interface roughness is expected to be small compared to the wavelength, making the SPM approach more valid. The SPM2 is also known to conserve energy [1], making it highly desirable for the computation of thermal emission. Energy conservation is achieved to second order in the SPM because the incoherent power contained in the first order Bragg scattered fields is compensated by a second order reduction in the power of the coherent fields.

In this paper, we examine and confirm SPM2's energy conservation when predicting scattering and thermal emission from multilayer 1D rough interfaces. The SPM2 formulation is reviewed using a coupled Lippmann-Schwinger equations derived from Green's theorem. The zeroth order, first order, and second order (coherent averaged) fields are solved recursively. A recursive method is used so that SPM2 can be applied to a large number of rough interfaces without high computational cost and memory requirements.

The resulting zeroth order solution represents the flat surface coherent specularly reflected and transmitted fields of the multilayer structure, while the first order solution captures the incoherent Bragg scattered and transmitted fields scattered into all directions. The second order correction to the coherent fields is determined through an integration over wavenumber k_x that includes both "propagating" and "evanescent" values for k_x. The final total reflected and transmitted powers are expressed as a sum of integrations over k_x for each interface, with each including the surface power spectral density weighted by a kernel function which corresponds to power spectral density of wave propagation. The resulting kernel functions show that energy conservation is obeyed for any dielectric contrast, any layer configuration and interface, and arbitrary roughness spectra.

The paper is organized as follows. In Section 2, we formulate the coupled Lippmann-Schwinger equations in the spectral domain and derive the bistatic scattering and transmission coefficients for multilayer rough interface scattering problem. A recursive method of solving the surface fields is given in Section 3 which is useful for a large number of rough interfaces. Section 4 illustrates the numerical simulation results. Section 5 concludes this paper. The derivation of Lippmann-Schwinger equation, scattering potentials, and the solution of surface fields, as well as scattered and transmitted fields and powers, are given in the appendices.

2. FORMULATION

2.1. Formulation using Extinction Theorem

We use extinction theorems to formulate the integral equations. Consider the multilayer structure shown in Figure 1, there are $n+1$ regions separated by n rough interfaces at different depths. The lth rough boundary is denoted by $z = -d_l + f_l(x)$, with $d_0 = 0$. The permittivity and permeability of region l are denoted by ε_l, μ_l.

Consider a wave incident from region 0 upon the rough surfaces:

$$\psi_{inc}(x,z) = \int_{-\infty}^{\infty} dk_x e^{ik_x x - ik_z z} \tilde{\psi}_{inc}(k_x) \tag{1}$$

where $\tilde{\psi}_{inc}(k_x)$ represents the amplitude of any incident wave and $k_z = \sqrt{k_0^2 - k_x^2}$. For plane wave

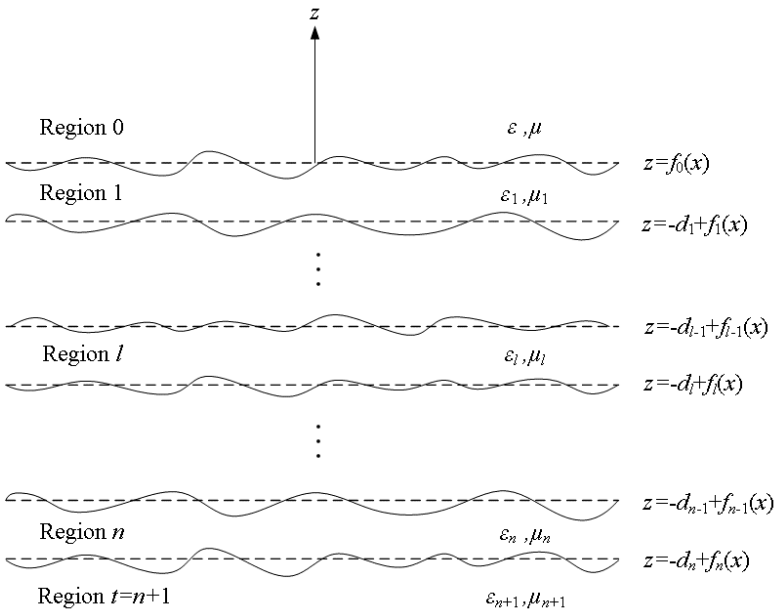

Figure 1. Geometry of layered medium with rough interfaces.

incidence,

$$\psi_{inc}(x,z) = e^{ik_{ix}x - ik_{iz}z} \tag{2}$$

By applying Green's theorem [32] to region 0, we obtain the integral equation

$$\psi_{inc}(\bar{r}) + \int_{S_0'} ds' \hat{n}_0' \cdot \left[\psi_0(\bar{r}') \nabla g_0(\bar{r},\bar{r}') - g_0(\bar{r},\bar{r}') \nabla \psi_0(\bar{r}')\right] = \begin{cases} \psi_0(\bar{r}) & \bar{r} \text{ in region } 0 \\ 0 & \bar{r} \text{ in region } 1 \end{cases} \tag{3}$$

By using Green's theorem to region l, the integral equation is

$$\begin{aligned} &\int_{S_{l-1}'} ds' \hat{n}_{l-1}' \cdot \left[\psi_{l-1}(\bar{r}') \nabla g_l(\bar{r},\bar{r}') - g_l(\bar{r},\bar{r}') \nabla \psi_{l-1}(\bar{r}')\right] \\ &- \int_{S_l'} ds' \hat{n}_l' \cdot \left[\psi_l(\bar{r}') \nabla g_l(\bar{r},\bar{r}') - g_l(\bar{r},\bar{r}') \nabla \psi_l(\bar{r}')\right] = \begin{cases} 0 & \bar{r} \text{ in region } l-1 \\ \psi_l(\bar{r}) & \bar{r} \text{ in region } l \\ 0 & \bar{r} \text{ in region } l+1 \end{cases} \end{aligned} \tag{4}$$

By applying Green's theorem to region $n+1$, the integral equation is

$$\int_{S_n'} ds' \hat{n}_n' \cdot \left[\psi_n(\bar{r}') \nabla g_{n+1}(\bar{r},\bar{r}') - g_{n+1}(\bar{r},\bar{r}') \nabla \psi_n(\bar{r}')\right] = \begin{cases} 0 & \bar{r} \text{ in region } n \\ \psi_t(\bar{r}) & \bar{r} \text{ in region } n+1 \end{cases} \tag{5}$$

Note that we have $2n+2$ equations from the extinction theorem (1 equation from top region, 2 equations from each intermediate region (totally n regions), and 1 from bottom region). The coupled equations are used to solve the surface fields on the $n+1$ boundaries. There are $2n+2$ surface unknowns for zeroth order and $2n+2$ boundary conditions. After solving the surface fields recursively, the scattered and transmitted fields can be solved from Equations (3) and (5) by putting observation point in region 0 or region $n+1$, respectively.

The 2D Green's function in region l is $g_l(\bar{r},\bar{r}') = \frac{i}{4} H_0^{(1)}\left(k_l \sqrt{(x-x')^2 + (z-z')^2}\right)$, with spectral representation given by

$$g_l(\bar{r},\bar{r}') = \frac{i}{4\pi} \int_{-\infty}^{\infty} dk_x \frac{1}{k_{lz}} e^{ik_x(x-x') + ik_{lz}|z-z'|} \tag{6}$$

where $k_{lz} = \sqrt{k_l^2 - k_x^2}$ and k_l is the wave number in region l.

We define surface unknowns as

$$\begin{aligned} a_l\left(x'\right) &= \psi_l(x', z' = -d_l + f_l(x')) \\ b_l\left(x'\right) &= \sqrt{1+\left[\frac{df_l(x')}{dx'}\right]^2}\,\hat{n}'\cdot\bar{\nabla}'\psi_l(x', z'=-d_l+f_l(x')) \end{aligned} \tag{7}$$

The boundary conditions on the lth rough interface $z' = -d_l + f_l(x')$ are

$$\begin{aligned} a_{l+1}\left(x'\right) &= a_l\left(x'\right) \\ b_{l+1}\left(x'\right) &= \frac{1}{\rho_{l,l+1}} b_l\left(x'\right) \end{aligned} \tag{8}$$

where $\rho_{l,l+1} = \frac{\varepsilon_l}{\varepsilon_{l+1}}$ for TM polarization and $\rho_{l,l+1} = \frac{\mu_l}{\mu_{l+1}}$ for TE polarization.

Surface fields in the spectral domain are

$$\begin{aligned} A_l\left(k_x\right) &= \frac{1}{2\pi}\int_{-\infty}^{\infty} dx' e^{-ik_x x'} a_l\left(x'\right) \\ B_l\left(k_x\right) &= \frac{1}{2\pi}\int_{-\infty}^{\infty} dx' e^{-ik_x x'} b_l\left(x'\right) \end{aligned} \tag{9}$$

Substituting the spectral green's function and the spectral domain surface fields into the coupled equations, we obtain the Lippmann-Schwinger equations in the spectral domain.

The equation for region 0 is

$$-\frac{1}{2}A_0\left(k_x\right) - \int_{-\infty}^{\infty} dk_x' V_{00}^{N-}\left(k_x, k_x'\right) A_0\left(k_x'\right) - \frac{i}{2}\frac{1}{k_{0z}} B_0\left(k_x\right) - \int_{-\infty}^{\infty} dk_x' V_{00}^{D-}\left(k_x, k_x'\right) B_0\left(k_x'\right) = -\delta(k_x - k_{ix}) \tag{10}$$

The coupled equations for region l are

$$\begin{aligned} &\frac{1}{2}e^{ik_{lz}d_{l-1}} A_{l-1}\left(k_x\right) + \int_{-\infty}^{\infty} dk_x' V_{l,l-1}^{N+}\left(k_x, k_x'\right) A_{l-1}\left(k_x'\right) - \frac{i}{2}\frac{1}{k_{lz}}\frac{1}{\rho_{l-1,l}} e^{ik_{lz}d_{l-1}} B_{l-1}\left(k_x\right) \\ &- \int_{-\infty}^{\infty} dk_x' V_{l,l-1}^{D+}\left(k_x, k_x'\right) B_{l-1}\left(k_x'\right) - \frac{1}{2}e^{ik_{lz}d_l} A_l\left(k_x\right) - \int_{-\infty}^{\infty} dk_x' V_{l,l}^{N+}\left(k_x, k_x'\right) A_l\left(k_x'\right) \\ &+ \frac{i}{2}\frac{1}{k_{lz}} e^{ik_{lz}d_l} B_l\left(k_x\right) + \int_{-\infty}^{\infty} dk_x' V_{l,l}^{D+}\left(k_x, k_x'\right) B_l\left(k_x'\right) = 0 \\ &- \frac{1}{2}e^{-ik_{lz}d_{l-1}} A_{l-1}\left(k_x\right) - \int_{-\infty}^{\infty} dk_x' V_{l,l-1}^{N-}\left(k_x, k_x'\right) A_{l-1}\left(k_x'\right) - \frac{i}{2}\frac{1}{k_{lz}}\frac{1}{\rho_{l-1,l}} e^{-ik_{lz}d_{l-1}} B_{l-1}\left(k_x\right) \\ &- \int_{-\infty}^{\infty} dk_x' V_{l,l-1}^{D-}\left(k_x, k_x'\right) B_{l-1}\left(k_x'\right) + \frac{1}{2}e^{-ik_{lz}d_l} A_l\left(k_x\right) + \int_{-\infty}^{\infty} dk_x' V_{l,l}^{N-}\left(k_x, k_x'\right) A_l\left(k_x'\right) \\ &+ \frac{i}{2}\frac{1}{k_{lz}} e^{-ik_{lz}d_l} B_l\left(k_x\right) + \int_{-\infty}^{\infty} dk_x' V_{l,l}^{D-}\left(k_x, k_x'\right) B_l\left(k_x'\right) = 0 \end{aligned} \tag{11}$$

And the equation for region $n+1$ is

$$\begin{aligned} &\frac{1}{2}e^{ik_{(n+1)z}d_n} A_n\left(k_x\right) + \int_{-\infty}^{\infty} dk_x' V_{n+1,n}^{N+}\left(k_x, k_x'\right) A_n\left(k_x'\right) - \frac{i}{2}\frac{1}{k_{(n+1)z}}\frac{1}{\rho_{n,n+1}} e^{ik_{(n+1)z}d_n} B_n\left(k_x\right) \\ &- \int_{-\infty}^{\infty} dk_x' V_{n+1,n}^{D+}\left(k_x, k_x'\right) B_n\left(k_x'\right) = 0 \end{aligned} \tag{12}$$

The detailed derivations of Lippmann-Schwinger equations are given in Appendix A. The scattering potentials are listed in Appendix B.1.

2.2. Small Perturbation Theory and Surface Fields Solutions

The second order small perturbation method solves the coupled spectral domain equations in a recursive manner up to second order.

To solve the surface fields, the perturbation method makes use of series expansions up to second order. Let

$$\begin{aligned} A_l(k_x) &= A_l^{(0)}(k_x) + A_l^{(1)}(k_x) + A_l^{(2)}(k_x) \\ B_l(k_x) &= B_l^{(0)}(k_x) + B_l^{(1)}(k_x) + B_l^{(2)}(k_x) \end{aligned} \tag{13}$$

In this paper, we only solve zeroth, first and coherent averaged second order surface fields because it is demonstrated that energy conservation for second order power is obeyed, irrespective of the roughness parameters.

An assumption of the smallness of the surface height is used to balance the order of solutions. The scattering potentials can be expressed in first and second orders according to Appendix B.2.

$$V_{p,q}(k_x,k_x') = V_{p,q}^{(1)}(k_x,k_x') + V_{p,q}^{(2)}(k_x,k_x') \tag{14}$$

Then by balancing the zeroth order of the Lippmann-Schwinger equations, the zeroth order surface fields are obtained as

$$\bar{U}^{(0)} = \bar{U}_C^{(0)}\delta(k_x - k_{ix}) \tag{15}$$

Mathematically, there is no scattering potential of the rough interfaces included in zeroth order coupled equations. Physically, the zeroth order solution is the exact solution for a multilayer medium with flat interfaces.

By balancing the first order of the Lippmann-Schwinger equations and substituting the zeroth order surface fields and first order scattering potentials, the first order surface fields are obtained as a summation of Fourier transforms multiplied by Fourier coefficients as follows

$$\bar{U}^{(1)} = \bar{\bar{U}}_C^{(1)}\bar{F} \tag{16}$$

where $\bar{\bar{U}}_C^{(1)}$ is the Fourier coefficients matrix, and $\bar{F}$ is the vector of aligned Fourier transforms of each rough interface.

By balancing the second order of the Lippmann-Schwinger equations, the second order surface fields after coherent averaging are obtained as follows.

$$< \bar{U}^{(2)} > = < \bar{\bar{U}}_C^{(2)} > \bar{W}\delta(k_x - k_{ix}) \tag{17}$$

where $\bar{\bar{U}}_C^{(2)}$ is the spectral density coefficients matrix, and $\bar{W}$ is the vector of aligned spectral densities of each rough interface. The detailed matrix forms and direct-inverting method are given in Appendix C.

Physically, the zeroth order solution is found as same as the case with flat interfaces. The first order solution can be interpreted as a Bragg scattering modulation from incident direction to arbitrary direction determined by k_x. The second order solution can be interpreted as a double modulation of scattering by the rough interface, the coherent averaging of which gives a Dirac delta function.

To apply this method to the case of a large number of rough interfaces, a recursive method is proposed in Section 3, which cascades the top and bottom surface fields and thus reduces the computational cost and memory requirement.

2.3. Bistatic Scattering and Transmission Coefficients

Putting the observation point in region 0 and region $n+1$ and expressing the integral Equations (3) and (5) into their spectral domain forms produce

$$\psi_s(k_x) = \frac{1}{2}A_0(k_x) + \int_{-\infty}^{\infty} dk_x' V_{00}^{N+}(k_x,k_x') A_0(k_x') - \frac{i}{2}\frac{1}{k_{0z}}B_0(k_x) - \int_{-\infty}^{\infty} dk_x' V_{00}^{D+}(k_x,k_x') B_0(k_x') \tag{18}$$

$$\begin{aligned}\psi_t\left(k_x\right) &= \frac{1}{2}e^{-ik_{(n+1)z}d_n}A_n\left(k_x\right)+\int_{-\infty}^{\infty}dk_x'V_{n+1,n}^{N-}\left(k_x,k_x'\right)A_n\left(k_x'\right)\\ &+\frac{i}{2}\frac{1}{k_{(n+1)z}}\frac{1}{\rho_{n,n+1}}e^{-ik_{(n+1)z}d_n}B_n\left(k_x\right)+\int_{-\infty}^{\infty}dk_x'V_{n+1,n}^{D-}\left(k_x,k_x'\right)B_n\left(k_x'\right)\end{aligned} \tag{19}$$

Substituting surface fields and scattering potentials of the top and bottom rough surfaces, we obtain zeroth to second order scattered and transmitted fields. The simplified solutions are given below, while detailed solutions are listed in Appendix D.1.

The zeroth order solution is a product of a coefficient and a delta function.

$$\begin{aligned}\psi_s^{(0)}\left(k_x\right)&=\tilde{\psi}_s^{(0)}\left(k_x\right)\delta(k_x-k_{ix})\\ \psi_t^{(0)}\left(k_x\right)&=\tilde{\psi}_t^{(0)}\left(k_x\right)\delta(k_x-k_{tix})\end{aligned} \tag{20}$$

where k_{ix} denotes the specular reflection direction, and k_{tix} denotes the specular transmission direction.

The first order solution is a summation of the Fourier transforms of the rough interfaces with differing amplitudes $\tilde{\psi}_{sl}^{(1)}\left(k_x\right)$ (determined by the layered medium properties and scattering geometry)

$$\begin{aligned}\psi_s^{(1)}\left(k_x\right)&=\sum_{l=0}^{n}\tilde{\psi}_{sl}^{(1)}\left(k_x,k_{ix}\right)F_l(k_x-k_{ix})\\ \psi_t^{(1)}\left(k_x\right)&=\sum_{l=0}^{n}\tilde{\psi}_{tl}^{(1)}\left(k_x,k_{ix}\right)F_l\left(k_x-k_{ix}\right)\end{aligned} \tag{21}$$

Note that the coherent averaging of two Fourier transforms gives a delta function when the roughnesses on distinct interfaces are assumed to be uncorrelated:

$$<F_p(k_x-k_x')F_q(k_x'-k_{ix})>=\begin{cases}\delta(k_x-k_{ix})W_p(k_x'-k_{ix}) & p=q\\ 0 & p\neq q\end{cases} \tag{22}$$

The second order solution is a summation of the product of two arbitrary Fourier transforms of the rough interfaces with individual coefficients. When calculating the second order power, only the coherent averaged second order fields are needed. After coherent averaging, only those products of same Fourier transforms are left

$$\begin{aligned}<\psi_s^{(2)}(k_x)>&=\delta(k_x-k_{ix})\int_{-\infty}^{\infty}dk_x'\sum_{l=0}^{n}\tilde{\psi}_{sl}^{(2)}\left(k_x',k_{ix}\right)W_l(k_x'-k_{ix})\\ <\psi_t^{(2)}(k_x)>&=\delta(k_x-k_{tix})\int_{-\infty}^{\infty}dk_x'\sum_{l=0}^{n}\tilde{\psi}_{tl}^{(2)}\left(k_x',k_{ix}\right)W_l(k_x'-k_{ix})\end{aligned} \tag{23}$$

The reflected and transmitted powers are calculated from the surface fields, up to second order. The detailed derivations are given in Appendix D.2. Normalized by the incident power, the total coherent and incoherent scattering and transmission coefficients are obtained as follows, for TM polarization,

$$\begin{aligned}\gamma_{coh}^{TM}(\theta_i,\theta_s^{spec})&=\left\{\left|\tilde{\psi}_s^{(0)}\left(k_{ix}\right)\right|^2+2\mathrm{Re}\left[\tilde{\psi}_s^{(0)}\left(k_{ix}\right)\int_{-\infty}^{\infty}dk_x\sum_{l=0}^{n}\tilde{\psi}_{sl}^{(2)}\left(k_x,k_{ix}\right)W_l(k_x-k_{ix})\right]\right\}\\ \tau_{coh}^{TM}(\theta_i,\theta_t^{spec})&=\sqrt{\frac{\varepsilon_0}{\varepsilon_{n+1}}}\frac{\cos\theta_t^{spec}}{\cos\theta_i}\left\{\left|\tilde{\psi}_t^{(0)}(k_{ix})\right|^2+2\mathrm{Re}\left[\tilde{\psi}_t^{(0)}(k_{ix})\int_{-\infty}^{\infty}dk_x\sum_{l=0}^{n}\tilde{\psi}_{tl}^{(2)}(k_x,k_{ix})W_l(k_x-k_{ix})\right]\right\}\\ \gamma_{incoh}^{TM}(\theta_i,\theta_s)&=\int_{-\pi/2}^{\pi/2}d\theta_s k_0\frac{\cos^2\theta_s}{\cos\theta_i}\sum_{l=0}^{n}\left|\tilde{\psi}_{sl}^{(1)}\left(k_x,k_{ix}\right)\right|^2W_l(k_x-k_{ix})\\ \tau_{incoh}^{TM}(\theta_i,\theta_t)&=\int_{-\pi/2}^{\pi/2}d\theta_t k_0\frac{\cos^2\theta_t}{\cos\theta_i}\sum_{l=0}^{n}\left|\tilde{\psi}_{tl}^{(1)}\left(k_x,k_{ix}\right)\right|^2W_l(k_x-k_{ix})\end{aligned} \tag{24}$$

where γ and τ are scattering and transmission coefficients, respectively; θ_s^{spec} and θ_t^{spec} are the specular reflection and transmission angles, respectively, determined by the incident angle and the permittivities of top and bottom medium, $\theta_s^{spec} = \theta_i$, $\theta_t^{spec} = \sin^{-1}(\sqrt{\frac{\varepsilon_0}{\varepsilon_{n+1}}}\sin\theta_i)$, according to Snell's law. The coherent waves are in the specular directions while the incoherent waves are in all directions from $-\pi/2$ to $\pi/2$.

And for TE polarization,

$$\begin{aligned}
\gamma_{coh}^{TE}(\theta_i,\theta_s^{spec}) &= \left\{\left|\tilde{\psi}_s^{(0)}(k_{ix})\right|^2 + 2\mathrm{Re}\left[\tilde{\psi}_s^{(0)}(k_{ix})\int_{-\infty}^{\infty}dk_x\sum_{l=0}^{n}\tilde{\psi}_{sl}^{(2)}(k_x,k_{ix})\,W_l(k_x-k_{ix})\right]\right\}\\
\tau_{coh}^{TE}(\theta_i,\theta_t^{spec}) &= \sqrt{\frac{\varepsilon_{n+1}}{\varepsilon_0}}\frac{\cos\theta_t^{spec}}{\cos\theta_i}\left\{\left|\tilde{\psi}_t^{(0)}(k_{ix})\right|^2 + 2\mathrm{Re}\left[\tilde{\psi}_t^{(0)}(k_{ix})\int_{-\infty}^{\infty}dk_x\sum_{l=0}^{n}\tilde{\psi}_{tl}^{(2)}(k_x,k_{ix})W_l(k_x-k_{ix})\right]\right\}\\
\gamma_{incoh}^{TE}(\theta_i,\theta_s) &= \int_{-\pi/2}^{\pi/2}d\theta_s k_0\frac{\cos^2\theta_s}{\cos\theta_i}\sum_{l=0}^{n}\left|\tilde{\psi}_{sl}^{(1)}(k_x,k_{ix})\right|^2 W_l(k_x-k_{ix})\\
\tau_{incoh}^{TE}(\theta_i,\theta_t) &= \int_{-\pi/2}^{\pi/2}d\theta_t k_0\frac{\varepsilon_{n+1}}{\varepsilon_0}\frac{\cos^2\theta_t}{\cos\theta_i}\sum_{l=0}^{n}\left|\tilde{\psi}_{tl}^{(1)}(k_x,k_{ix})\right|^2 W_l(k_x-k_{ix})
\end{aligned} \tag{25}$$

2.4. SPM Kernel Functions of Power Spectral Densities

The zeroth order energy obeys energy conservation. The first order energy is zero because the averages of first order fields are zero. Thus change arises from second order energy.

The second order coherent energy is the average of the product of zeroth order field and complex conjugate of the second order field while the second order incoherent energy comes from the product of first order field and its complex conjugate. The former captures a decrease in the specularly reflected and transmitted powers, while the latter includes the Bragg scattered and transmitted powers in all bistatic directions. The combination of these terms should satisfy energy conservation for any dielectric contrast, any layer configuration and interface, and arbitrary roughness spectra. Thus we only need to examine the kernel functions as follows.

$$\begin{aligned}
r_{coh}^{(2)} &= \int_{-\infty}^{\infty}dk_x\sum_{l=0}^{n}R_{coh,l}^{(2)}(k_x,k_{ix})W_l(k_x-k_{ix})\\
t_{coh}^{(2)} &= \int_{-\infty}^{\infty}dk_x\sum_{l=0}^{n}T_{coh,l}^{(2)}(k_x,k_{ix})W_l(k_x-k_{ix})\\
r_{incoh}^{(2)} &= \int_{-k_0}^{k_0}dk_x\sum_{l=0}^{n}R_{incoh,l}^{(2)}(k_x,k_{ix})\,W_l(k_x-k_{ix})\\
t_{incoh}^{(2)} &= \int_{-k_{n+1}}^{k_{n+1}}dk_x\sum_{l=0}^{n}T_{incoh,l}^{(2)}(k_x,k_{ix})W_l(k_x-k_{ix})
\end{aligned} \tag{26}$$

where for lth rough interface

$$\begin{aligned}
R_{coh,l}^{(2)}(k_x,k_{ix}) &= \begin{cases} 2\mathrm{Re}\left[\tilde{\psi}_s^{(0)}(k_{ix})\,\tilde{\psi}_{sl}^{(2)}(k_x,k_{ix})\right] & \text{for } |k_x|\le k_0\\ 0 & \text{for } |k_x|>k_0\end{cases}\\
T_{coh,l}^{(2)}(k_x,k_{ix}) &= \begin{cases} 2\mathrm{Re}\left[\rho_{0,n+1}\frac{k_{(n+1)iz}}{k_{0iz}}\tilde{\psi}_t^{(0)}(k_{ix})\,\tilde{\psi}_{tl}^{(2)}(k_x,k_{ix})\right] & \text{for } |k_x|\le k_{n+1}\\ 0 & \text{for } |k_x|>k_{n+1}\end{cases}\\
R_{incoh,l}^{(2)}(k_x,k_{ix}) &= \mathrm{Re}\left[\frac{k_z^*}{k_{0iz}}\left|\tilde{\psi}_{sl}^{(1)}(k_x,k_{ix})\right|^2\right]
\end{aligned}$$

$$T^{(2)}_{incoh,l}\left(k_x,k_{ix}\right)=\mathrm{Re}\left[\rho_{0,n+1}\frac{k^*_{(n+1)z}}{k_{0iz}}\left|\tilde{\psi}^{(1)}_{tl}\left(k_x,k_{ix}\right)\right|^2\right] \tag{27}$$

where $\rho_{0,n+1}=\frac{\varepsilon_0}{\varepsilon_{n+1}}$ for TM polarization, $\rho_{0,n+1}=\frac{\mu_0}{\mu_{n+1}}$ for TE polarization.

It is noted that the incoherent waves arise only from the "propagating waves", i.e., for scattered wave $k_x\in[-k_0,k_0]$ while for transmitted wave $k_x\in[-k_{n+1},k_{n+1}]$. The coherent waves come from both the "propagating waves" and the "evanescent waves" where $k_x\in[-\infty,\infty]$. There are four kernel functions for each interface.

Then, since zeroth order energy conserves, the second order terms need to sum to zero to conserve energy as

$$r^{(2)}_{coh}+t^{(2)}_{coh}+r^{(2)}_{incoh}+t^{(2)}_{incoh}=0 \tag{28}$$

which means

$$\int_{-\infty}^{\infty}dk_x\sum_{l=0}^{n}\left[R^{(2)}_{coh,l}\left(k_x,k_{ix}\right)+T^{(2)}_{coh,l}\left(k_x,k_{ix}\right)+R^{(2)}_{incoh,l}\left(k_x,k_{ix}\right)+T^{(2)}_{incoh,l}\left(k_x,k_{ix}\right)\right]W_l(k_x-k_{ix})=0 \tag{29}$$

The above seems to be complicated because it seems that one has to specify all $W_l\left(k_x-k_{ix}\right)$ $(l=0,1,\ldots,n)$, substitute kernel functions and roughness spectral densities, sum from 0 to n, and integrate from $-\infty$ to ∞ to get 0. The key result we show in this paper is that this is not necessary as we show the much stronger condition that

$$R^{(2)}_{coh,l}\left(k_x,k_{ix}\right)+T^{(2)}_{coh,l}\left(k_x,k_{ix}\right)+R^{(2)}_{incoh,l}\left(k_x,k_{ix}\right)+T^{(2)}_{incoh,l}\left(k_x,k_{ix}\right)=0 \tag{30}$$

for each k_x and each l.

We examine these kernel functions for a 2-layers case and a 51-layers case in Section 4. The detailed derivations are given in Appendix D.2.

3. RECURSIVE METHOD OF SOLVING THE COEFFICIENTS

The basic method to solve the surface fields is by inverting the matrix on the left hand side and multiplying with the right hand side of the equations. However, when the number of interfaces increases, the computational cost and requirement of memory will increase rapidly. A recursive method by cascading the surface fields of the top and bottom rough surfaces is used for fast computation.

The recursive relation can be derived from two coupled equations for each intermediate medium layer, and the key to this method is to develop a recursive relation between the unknowns of top and bottom surfaces.

Use the zeroth order solution as an example. For the lth medium, the coupled equations can be expressed as

$$\begin{aligned}
&\frac{1}{2}e^{ik_{lz}d_{l-1}}A^{(0)}_{l-1}\left(k_x\right)-\frac{i}{2}\frac{1}{k_{lz}}\frac{1}{\rho_{l-1,l}}e^{ik_{lz}d_{l-1}}B^{(0)}_{l-1}\left(k_x\right)-\frac{1}{2}e^{ik_{lz}d_l}A^{(0)}_{l}\left(k_x\right)+\frac{i}{2}\frac{1}{k_{lz}}e^{ik_{lz}d_l}B^{(0)}_{l}\left(k_x\right)=0\\
&-\frac{1}{2}e^{-ik_{lz}d_{l-1}}A^{(0)}_{l-1}\left(k_x\right)-\frac{i}{2}\frac{1}{k_{lz}}\frac{1}{\rho_{l-1,l}}e^{-ik_{lz}d_{l-1}}B^{(0)}_{l-1}\left(k_x\right)+\frac{1}{2}e^{-ik_{lz}d_l}A^{(0)}_{l}\left(k_x\right)\\
&+\frac{i}{2}\frac{1}{k_{lz}}e^{-ik_{lz}d_l}B^{(0)}_{l}\left(k_x\right)=0
\end{aligned} \tag{31}$$

The recursive relation can be expressed in a matrix form as

$$\begin{bmatrix}A^{(0)}_{l}\left(k_x\right)\\B^{(0)}_{l}\left(k_x\right)\end{bmatrix}=\bar{\bar{M}}_{l,l-1}\begin{bmatrix}A^{(0)}_{l-1}\left(k_x\right)\\B^{(0)}_{l-1}\left(k_x\right)\end{bmatrix} \tag{32}$$

where

$$\bar{\bar{M}}_{l,l-1}=\frac{1}{2}\begin{bmatrix}e^{ik_{lz}t_l}+e^{-ik_{lz}t_l} & \frac{i}{k_{lz}}\frac{1}{\rho_{l-1,l}}\left(e^{ik_{lz}t_l}-e^{-ik_{lz}t_l}\right)\\ -ik_{lz}\left(e^{ik_{lz}t_l}-e^{-ik_{lz}t_l}\right) & \frac{1}{\rho_{l-1,l}}\left(e^{ik_{lz}t_l}+e^{-ik_{lz}t_l}\right)\end{bmatrix}$$

where $t_l = d_l - d_{l-1}$ is the thickness of the lth medium.

Using this recursive relation, we can relate the surface fields on the top surface to the surface fields on the bottom surface.

$$\begin{bmatrix} A_n^{(0)}(k_x) \\ B_n^{(0)}(k_x) \end{bmatrix} = \left[\prod_{l=1}^{n} \bar{\bar{M}}_{l,l-1}\right] \begin{bmatrix} A_0^{(0)}(k_x) \\ B_0^{(0)}(k_x) \end{bmatrix} \tag{33}$$

Substitute in the two equations for top and bottom surfaces

$$\begin{aligned} &-\frac{1}{2}A_0^{(0)}(k_x) - \frac{i}{2}\frac{1}{k_{0z}}B_0^{(0)}(k_x) = -1 \\ &\frac{1}{2}e^{ik_{(n+1)z}d_n}A_n^{(0)}(k_x) - \frac{i}{2}\frac{1}{k_{nz}}\frac{1}{\rho_{n,n+1}}e^{ik_{(n+1)z}d_n}B_n^{(0)}(k_x) = 0 \end{aligned} \tag{34}$$

We only need to invert a 2×2 matrix to obtain the zeroth order surface fields solution on top and bottom surfaces. Then we can compute the surface field solutions of all rough interfaces. The solution agrees with that computed from matrix inverting method.

The recursive relation of first order fields for the lth medium is

$$\begin{bmatrix} A_l^{(1)}(k_x) \\ B_l^{(1)}(k_x) \end{bmatrix} = \bar{\bar{M}}_{l,l-1}\begin{bmatrix} A_{l-1}^{(1)}(k_x) \\ B_{l-1}^{(1)}(k_x) \end{bmatrix} + \bar{\bar{V}}_{l,l-1}^{(1)}\begin{bmatrix} A_{l-1}^{(0)}(k_x) \\ B_{l-1}^{(0)}(k_x) \end{bmatrix} F_{l-1}(k_x - k_{ix}) + \bar{\bar{V}}_{l,l}^{(1)}\begin{bmatrix} A_l^{(0)}(k_x) \\ B_l^{(0)}(k_x) \end{bmatrix} F_l(k_x - k_{ix}) \tag{35}$$

where the first order scattering potential matrices are

$$\begin{aligned} \bar{\bar{V}}_{l,l-1}^{(1)} &= \begin{bmatrix} -\left(e^{ik_{lz}t_l} - e^{-ik_{lz}t_l}\right)\tilde{V}_{l,l-1}^{N+(1)}(k_x,k_{ix}) & -\left(e^{ik_{lz}t_l} + e^{-ik_{lz}t_l}\right)\tilde{V}_{l,l-1}^{D+(1)}(k_x,k_{ix}) \\ ik_{lz}\left(e^{ik_{lz}t_l} + e^{-ik_{lz}t_l}\right)\tilde{V}_{l,l-1}^{N+(1)}(k_x,k_{ix}) & ik_{lz}\left(e^{ik_{lz}t_l} - e^{-ik_{lz}t_l}\right)\tilde{V}_{l,l-1}^{D+(1)}(k_x,k_{ix}) \end{bmatrix} \\ \bar{\bar{V}}_{l,l}^{(1)} &= \begin{bmatrix} 0 & 2e^{-ik_{lz}t_l}\tilde{V}_{l,l}^{D+(1)}(k_x,k_{ix}) \\ -2ik_{lz}e^{-ik_{lz}t_l}\tilde{V}_{l,l}^{N+(1)}(k_x,k_{ix}) & 0 \end{bmatrix} \end{aligned} \tag{36}$$

The recursive relation of second order fields for the lth medium is

$$\begin{aligned} &\begin{bmatrix} <A_l^{(2)}(k_x)> \\ <B_l^{(2)}(k_x)> \end{bmatrix} = \bar{\bar{M}}_{l,l-1}\begin{bmatrix} A_{l-1}^{(2)}(k_x) \\ B_{l-1}^{(2)}(k_x) \end{bmatrix} + <\bar{\bar{V}}_{l,l-1}^{(2)}>\begin{bmatrix} A_{l-1}^{(0)}(k_x) \\ B_{l-1}^{(0)}(k_x) \end{bmatrix} W_{l-1}(k_x - k_{ix}) \\ &+ <\bar{\bar{V}}_{l,l}^{(2)}>\begin{bmatrix} A_l^{(0)}(k_x) \\ B_l^{(0)}(k_x) \end{bmatrix} W_l(k_x - k_{ix}) + <\bar{\bar{V}}_{l,l-1}^{(1)}>\begin{bmatrix} A_{l-1}^{(1)}(k_x) \\ B_{l-1}^{(1)}(k_x) \end{bmatrix} W_{l-1}(k_x - k_{ix}) \\ &+ <\bar{\bar{V}}_{l,l}^{(1)}>\begin{bmatrix} A_l^{(1)}(k_x) \\ B_l^{(1)}(k_x) \end{bmatrix} W_l(k_x - k_{ix}) \end{aligned} \tag{37}$$

where the first order scattering potential matrices operate with the first order surface fields, the second order scattering potential matrices operate with the zeroth order surface fields, and both of them contribute to the second order fields. The second order scattering potential matrices are

$$\begin{aligned} \bar{\bar{V}}_{l,l-1}^{(2)} &= \begin{bmatrix} \left(e^{ik_{lz}t_l} + e^{-ik_{lz}t_l}\right)\tilde{V}_{l,l-1}^{N+(2)}(k_x,k_{ix}) & \left(e^{ik_{lz}t_l} - e^{-ik_{lz}t_l}\right)\tilde{V}_{l,l-1}^{D+(2)}(k_x,k_{ix}) \\ -ik_{lz}\left(e^{ik_{lz}t_l} - e^{-ik_{lz}t_l}\right)\tilde{V}_{l,l-1}^{N+(2)}(k_x,k_{ix}) & -ik_{lz}\left(e^{ik_{lz}t_l} + e^{-ik_{lz}t_l}\right)\tilde{V}_{l,l-1}^{D+(2)}(k_x,k_{ix}) \end{bmatrix} \\ \bar{\bar{V}}_{l,l}^{(2)} &= \begin{bmatrix} -2e^{-ik_{lz}t_l}\tilde{V}_{l,l}^{D+(1)}(k_x,k_{ix}) & 0 \\ 0 & 2ik_{lz}e^{-ik_{lz}t_l}\tilde{V}_{l,l}^{N+(1)}(k_x,k_{ix}) \end{bmatrix} \end{aligned} \tag{38}$$

Equations (36), (38) are simplified scattering potential matrices by using $\tilde{V}_{p,q}^{N+(1)} = -\tilde{V}_{p,q}^{N-(1)}$, $\tilde{V}_{p,q}^{D+(1)} = -\tilde{V}_{p,q}^{D-(1)}$, $\tilde{V}_{p,q}^{N+(2)} = \tilde{V}_{p,q}^{N-(2)}$, and $\tilde{V}_{p,q}^{D+(2)} = \tilde{V}_{p,q}^{D-(2)}$.

The recursive relation avoids the high computational costs of CPU and memory for inverting large matrix.

4. NUMERICAL RESULTS

Energy conservation is checked for both TM and TE polarizations for 2-layers and 51-layers cases. As shown in Section 2, scattering coefficients for reflection and transmission are expressed as an integration of the product of SPM kernel functions and surface spectral densities over the spectral domain. Energy conservation can therefore be examined using the SPM kernel functions without any specification of the surface roughness. Note the fact that energy conservation is satisfied does not imply that the reflected or transmitted powers individually are accurate; they should be expected to be accurate only in the case of small surface heights relative to the electromagnetic wavelength.

4.1. Results for a 2-Layers Case

The parameters are as follows: frequency = 1.4 GHz, nadir incidence, layer thickness is 0.1 m, and the permittivities of region 0, region 1, and region 2 are 1, 1.4, and 2, respectively. SPM kernel functions for TM and TE polarizations are shown in Figures 2 and 3, respectively. The figures illustrate the

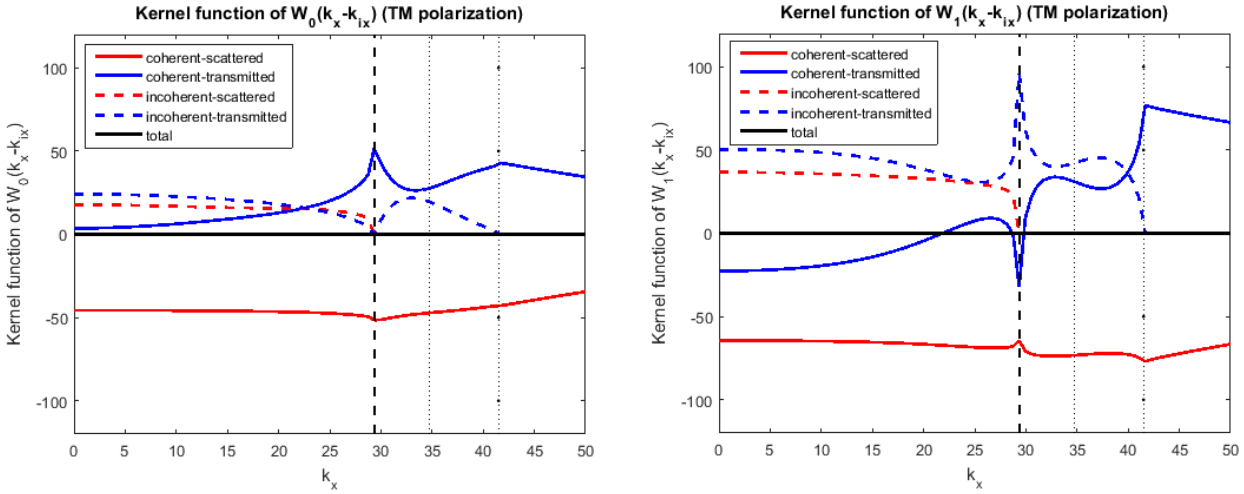

Figure 2. Kernel functions for TM polarization for 2-layers case, (a) W_0, (b) W_1.

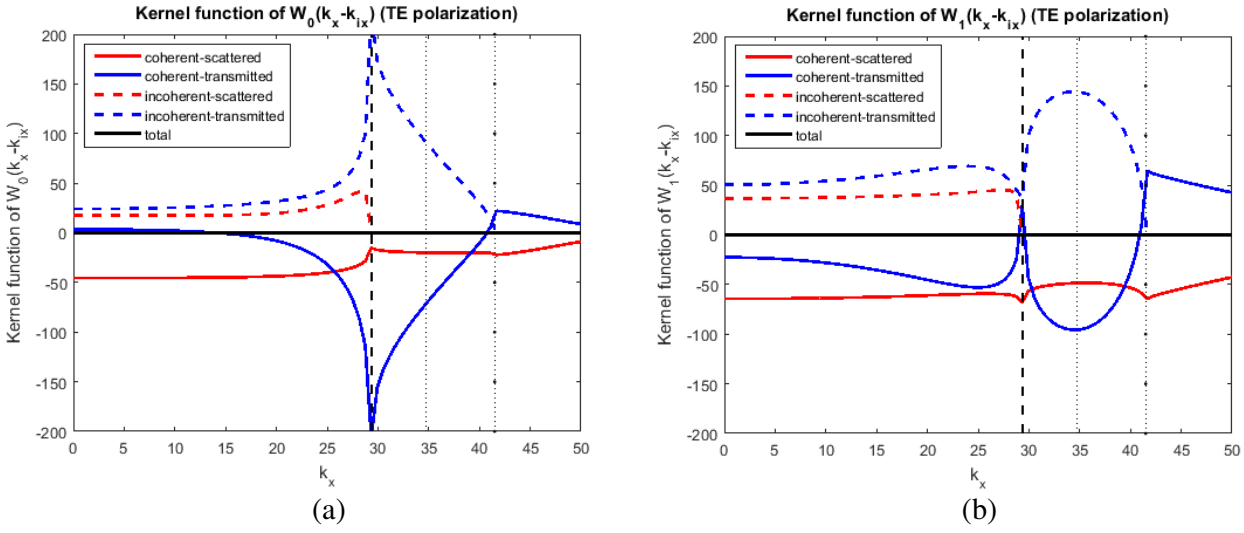

Figure 3. Kernel functions for TE polarization for 2-layers case, (a) W_0, (b) W_1.

coherent scattered and transmitted contributions, as well as the incoherent scattered and transmitted contributions, for the roughness of the upper interface (left plots) and for the roughness of the lower interface (right plots). The figures also include the sum of all contributions, which should equal zero if energy is conserved.

The sum results confirm energy conservation for the method as expected. Note that the incoherent scattered and transmitted waves have contributions only for $k_x < 29.3$ and $k_x < 41.5$, respectively, while the coherent contributions extend over the entire wavenumber range. When recombined to create an SPM kernel for emission (i.e., combining for example the reflected coherent and incoherent terms), the "critical phenomena" known to occur in microwave emission [33] arises, with distinct locations for the upper and lower interfaces. The SPM kernel functions for a given interface are dependent on the entire layered medium structure, and capture any "multi-bounce" interaction of the Bragg waves with the flat interfaces of the layered medium.

4.2. Results for a 51-Layers Case

The parameters are as follows: frequency = 1.4 GHz, the total number of rough interfaces is 51, and the layer thickness is 0.01 m for all layers. The wave approaches from nadir incidence. The top region permittivity is 1, the bottom region permittivity is 1.5, and the permittivities are of the form

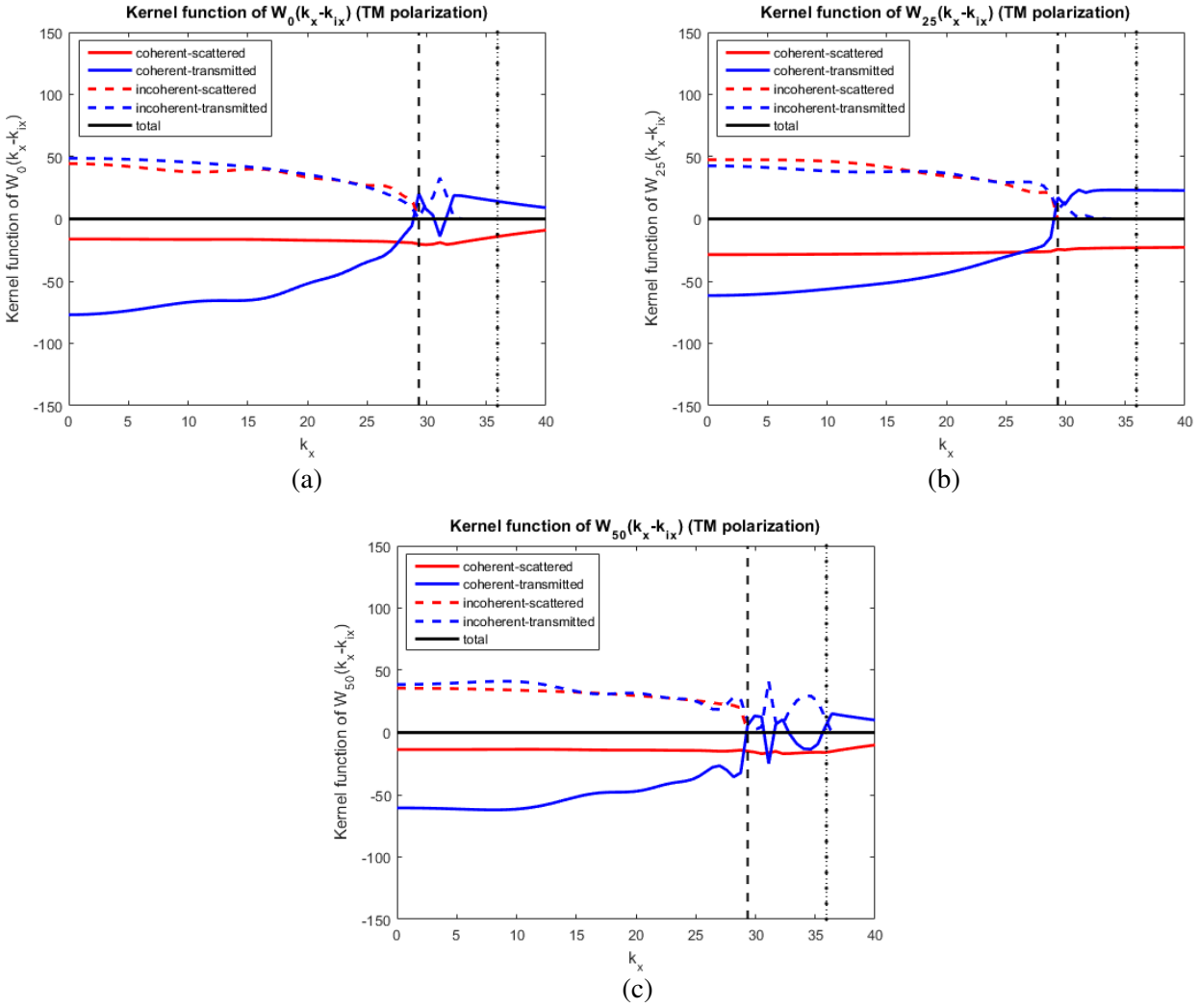

Figure 4. Kernel functions for TM polarization for 51-layers case, (a) W_0, (b) W_{25}, (c) W_{50}.

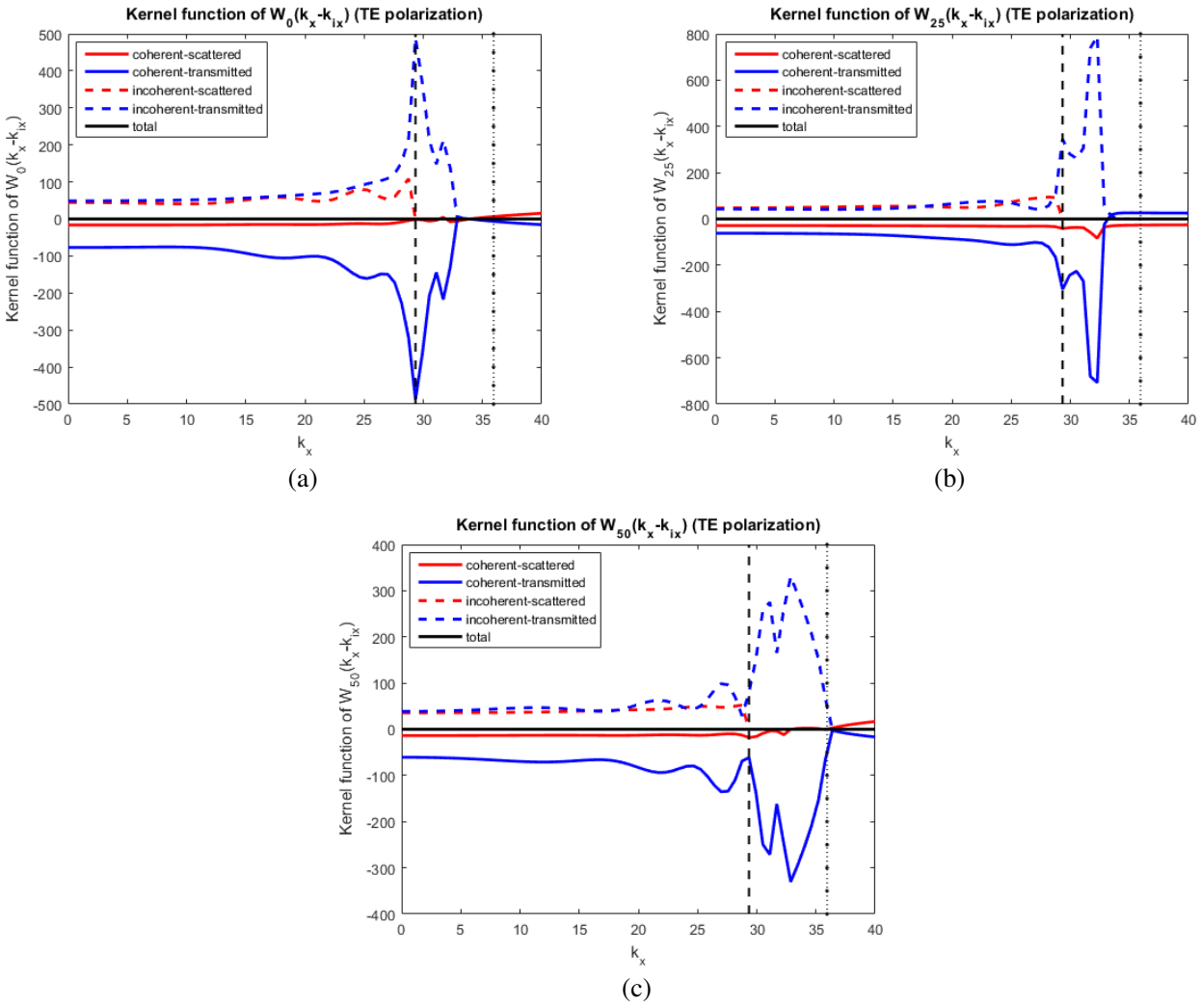

Figure 5. Kernel functions for TE polarization for 51-layers case, (a) W_0, (b) W_{25}, (c) W_{50}.

$[1, 1.5, 1, 1.5, \ldots, 1, 1.5, 1, 1.5]$ from top to bottom.

The SPM kernel functions for W_0, W_{25}, and W_{50} for TM and TE polarizations are shown in Figures 4 and 5, respectively.

The results again confirm energy conservation for the second order SPM.

5. CONCLUSION

This paper investigates the energy conservation of the second order small perturbation method. We develop a 2D multilayer SPM to calculate the bistatic scattering and transmission kernel functions of layered media with multiple 1D roughness. A recursive method to solve the surface fields up to second order is developed to save the computational cost of CPU and memory. The results were used to compute the SPM kernel functions for the total reflected and transmitted powers up to second order in the form of an integration over k_x of coherent and incoherent contributions for each interface. Energy conservation is confirmed in terms of the SPM kernel functions alone, so that the method is desirable for thermal emission computations. Numerical examples show that energy conservation is obeyed for any dielectric contrast, any layer configuration and interface, and arbitrary roughness spectra. Extensions to 3D cases are in process and will be reported in the future.

APPENDIX A. DERIVATION OF LIPPMANN-SCHWINGER EQUATIONS

The details of derivation of Lippmann-Schwinger equations in spectral domain are listed.

Substitute the spectral domain green's function to extinction theorem in Equations (3)–(5), we obtain the following coupled equations.

The equation for region 0 is

$$\int_{-\infty}^{\infty} dk_x e^{ik_x x - ik_{0z} z} \tilde{\psi}_{inc}(k_x) + \frac{i}{4\pi} \int_{-\infty}^{\infty} dk_x \frac{1}{k_{0z}} e^{ik_x x - ik_{0z} z} \times \int_{-\infty}^{\infty} dx' \left\{ a_0\left(x'\right) \left[ik_x \frac{df_0\left(x'\right)}{dx'} + ik_{0z} \right] - b_0\left(x'\right) \right\} \times e^{-ik_x x' + ik_{0z} f_0(x')} = 0 \tag{A1}$$

The equations for region l are

$$\begin{aligned} &\frac{i}{4\pi} \int_{-\infty}^{\infty} dk_x \frac{1}{k_{lz}} e^{ik_x x + ik_{lz} z} \int_{-\infty}^{\infty} dx' \left\{ a_{l-1}\left(x'\right) \left[ik_x \frac{df_{l-1}\left(x'\right)}{dx'} - ik_{lz} \right] - \frac{1}{\rho_{l-1,l}} b_{l-1}\left(x'\right) \right\} \\ &\times e^{-ik_x x' - ik_{lz}[-d_{l-1} + f_{l-1}(x')]} - \frac{i}{4\pi} \int_{-\infty}^{\infty} dk_x \frac{1}{k_{lz}} e^{ik_x x + ik_{lz} z} \int_{-\infty}^{\infty} dx' \left\{ a_l\left(x'\right) \left[ik_x \frac{df_l(x')}{dx'} - ik_{lz} \right] - b_l\left(x'\right) \right\} \\ &\times e^{-ik_x x' - ik_{lz}[-d_l + f_l(x')]} = 0 \\ &\frac{i}{4\pi} \int_{-\infty}^{\infty} dk_x \frac{1}{k_{lz}} e^{ik_x x - ik_{lz} z} \int_{-\infty}^{\infty} dx' \left\{ a_{l-1}\left(x'\right) \left[ik_x \frac{df_{l-1}\left(x'\right)}{dx'} + ik_{lz} \right] - \frac{1}{\rho_{l-1,l}} b_{l-1}\left(x'\right) \right\} \\ &\times e^{-ik_x x' + ik_{lz}[-d_{l-1} + f_{l-1}(x')]} - \frac{i}{4\pi} \int_{-\infty}^{\infty} dk_x \frac{1}{k_{lz}} e^{ik_x x - ik_{lz} z} \int_{-\infty}^{\infty} dx' \left\{ a_l\left(x'\right) \left[ik_x \frac{df_l(x')}{dx'} + ik_{lz} \right] - b_l\left(x'\right) \right\} \\ &\times e^{-ik_x x' + ik_{lz}[-d_l + f_l(x')]} = 0 \end{aligned} \tag{A2}$$

The equation for region $n+1$ is

$$\begin{aligned} &\frac{i}{4\pi} \int_{-\infty}^{\infty} dk_x \frac{1}{k_{(n+1)z}} e^{ik_x x + ik_{(n+1)z} z} \int_{-\infty}^{\infty} dx' \left\{ a_n\left(x'\right) \left[ik_x \frac{df_n\left(x'\right)}{dx'} - ik_{(n+1)z} \right] - \frac{1}{\rho_{n,n+1}} b_n\left(x'\right) \right\} \\ &\times e^{-ik_x x' - ik_{(n+1)z}[-d_n + f_n(x')]} = 0 \end{aligned} \tag{A3}$$

Using the Fourier transforms in Equation (9), we obtain the spectral domain equations. Substituting the scattering potentials listed in Appendix B.1, we obtain the coupled Lippmann-Schwinger equations as Equations (10)–(12).

APPENDIX B. SCATTERING POTENTIALS AND SMALL HEIGHT APPROXIMATION

B.1. Scattering Potentials

Four pairs of scattering potentials for lth region in Equation (11) are listed below.

The notations are: for the subscripts, first alphabet means the number of region, second alphabet means the number of rough interface; for the superscripts, N means Neumann boundary condition, D means Dirichlet boundary condition, and + means upward going wave, − means downward going wave.

$$\begin{aligned} V_{l,l-1}^{N+}\left(k_x,k_x'\right) &= \frac{1}{2k_{lz}^2} e^{ik_{lz} d_{l-1}} \left(k_l^2 - k_x k_x'\right) I_{l,l-1}^{+}\left(k_x,k_x'\right) \\ V_{l,l-1}^{D+}\left(k_x,k_x'\right) &= \frac{i}{2k_{lz}} \frac{1}{\rho_{l-1,l}} e^{ik_{lz} d_{l-1}} \left(k_l^2 - k_x k_x'\right) I_{l,l-1}^{+}\left(k_x,k_x'\right) \\ V_{l,l}^{N+}\left(k_x,k_x'\right) &= \frac{1}{2k_{lz}^2} e^{ik_{lz} d_l} \left(k_l^2 - k_x k_x'\right) I_{l,l}^{+}\left(k_x,k_x'\right) \\ V_{l,l}^{D+}(k_x,k_x') &= \frac{i}{2k_{lz}} e^{ik_{lz} d_l} \left(k_l^2 - k_x k_x'\right) I_{l,l}^{+}\left(k_x,k_x'\right) \end{aligned} \tag{B1}$$

where

$$\begin{aligned} I_{l,l-1}^{+}\left(k_x,k_x'\right) &= \frac{1}{2\pi}\int_{-\infty}^{\infty} dx' e^{-i(k_x-k_x')x'}[e^{-ik_{lz}f_{l-1}(x')}-1] \\ I_{l,l}^{+}\left(k_x,k_x'\right) &= \frac{1}{2\pi}\int_{-\infty}^{\infty} dx' e^{-i(k_x-k_x')x'}[e^{-ik_{lz}f_{l}(x')}-1] \end{aligned} \tag{B2}$$

Similarly,

$$\begin{aligned} V_{l,l-1}^{N-}\left(k_x,k_x'\right) &= \frac{1}{2k_{lz}^2}e^{-ik_{lz}d_{l-1}}\left(k_l^2-k_xk_x'\right)I_{l,l-1}^{-}\left(k_x,k_x'\right) \\ V_{l,l-1}^{D-}\left(k_x,k_x'\right) &= \frac{i}{2k_{lz}}\frac{1}{\rho_{l-1,l}}e^{-ik_{lz}d_{l-1}}\left(k_l^2-k_xk_x'\right)I_{l,l-1}^{-}\left(k_x,k_x'\right) \\ V_{l,l}^{N-}(k_x,k_x') &= \frac{1}{2k_{lz}^2}e^{-ik_{lz}d_{l}}\left(k_l^2-k_xk_x'\right)I_{l,l}^{-}\left(k_x,k_x'\right) \\ V_{l,l}^{D-}(k_x,k_x') &= \frac{i}{2k_{lz}}e^{-ik_{lz}d_{l}}\left(k_l^2-k_xk_x'\right)I_{l,l}^{-}\left(k_x,k_x'\right) \end{aligned} \tag{B3}$$

where

$$\begin{aligned} I_{l,l-1}^{-}\left(k_x,k_x'\right) &= \frac{1}{2\pi}\int_{-\infty}^{\infty} dx' e^{-i(k_x-k_x')x'}[e^{ik_{lz}f_{l-1}(x')}-1] \\ I_{l,l}^{-}\left(k_x,k_x'\right) &= \frac{1}{2\pi}\int_{-\infty}^{\infty} dx' e^{-i(k_x-k_x')x'}[e^{ik_{lz}f_{l}(x')}-1] \end{aligned} \tag{B4}$$

B.2. Small Height Approximation

To solve the SPM coupled equations for different orders, we need to specify the first and second order scattering potentials, which can be further calculated from the first and second order integration terms.

The small height approximation of the scattering potentials applies to Equations (B2), (B4).

The Fourier transform and inverse Fourier transform of the lth rough interface can be expressed as

$$\begin{aligned} F_l\left(k_x\right) &= \frac{1}{2\pi}\int_{-\infty}^{\infty} dx' e^{-ik_xx'}f_l\left(x'\right) \\ f_l\left(x'\right) &= \int_{-\infty}^{\infty} dk_x e^{ik_xx'}F_l\left(k_x\right) \end{aligned} \tag{B5}$$

The first order and second order expressions of the integration can be expressed as

$$\begin{aligned} I_{l,l-1}^{+(1)}\left(k_x,k_x'\right) &= -ik_{lz}F_{l-1}\left(k_x-k_x'\right) \\ I_{l,l-1}^{+(2)}\left(k_x,k_x'\right) &= -\frac{k_{lz}^2}{2}\int dk_x^{''}F_{l-1}\left(k_x-k_x'-k_x^{''}\right)F_{l-1}\left(k_x^{''}\right) \\ I_{l,l}^{+(1)}\left(k_x,k_x'\right) &= -ik_{lz}F_{l}\left(k_x-k_x'\right) \\ I_{l,l}^{+(2)}\left(k_x,k_x'\right) &= -\frac{k_{lz}^2}{2}\int dk_x^{''}F_{l}\left(k_x-k_x'-k_x^{''}\right)F_{l}\left(k_x^{''}\right) \\ I_{l,l-1}^{-(1)}\left(k_x,k_x'\right) &= ik_{lz}F_{l-1}\left(k_x-k_x'\right) \\ I_{l,l-1}^{-(2)}\left(k_x,k_x'\right) &= -\frac{k_{lz}^2}{2}\int dk_x^{''}F_{l-1}\left(k_x-k_x'-k_x^{''}\right)F_{l-1}\left(k_x^{''}\right) \\ I_{l,l}^{-(1)}\left(k_x,k_x'\right) &= ik_{lz}F_{l}\left(k_x-k_x'\right) \\ I_{l,l}^{-(2)}\left(k_x,k_x'\right) &= -\frac{k_{lz}^2}{2}\int dk_x^{''}F_{l}\left(k_x-k_x'-k_x^{''}\right)F_{l}\left(k_x^{''}\right) \end{aligned} \tag{B6}$$

Note that there is no need to generate surface profile and compute the Fourier transform. We only need to compute the Fourier coefficients.

APPENDIX C. MATRIX FORM SOLUTION OF SURFACE FIELDS

The zeroth order fields are solved by balancing the zeroth order terms of Equations (10)–(12).

The matrix form can be expressed as

$$\bar{\bar{Z}}^{(0)}\bar{U}^{(0)} = \bar{R}^{(0)} \tag{C1}$$

where $\bar{\bar{Z}}^{(0)}$ is a $(2n+2)\times(2n+2)$ matrix, $\bar{U}^{(0)}$ and $\bar{R}^{(0)}$ are $(2n+2)\times 1$ vectors. The unknown vector $\bar{U}^{(0)}$ is a combination of zeroth order solution for surface fields.

The zeroth order solution can be expressed as

$$\bar{U}^{(0)} = \bar{U}_C^{(0)}\delta\left(k_x - k_{ix}\right) \tag{C2}$$

where

$$\bar{U}_C^{(0)} = \left[\begin{array}{cccccccc} A_0^{(0)}\left(k_{ix}\right) & B_0^{(0)}\left(k_{ix}\right) & \cdots & A_l^{(0)}\left(k_{ix}\right) & B_l^{(0)}\left(k_{ix}\right) & \cdots & A_n^{(0)}\left(k_{ix}\right) & B_n^{(0)}\left(k_{ix}\right) \end{array}\right]^T \tag{C3}$$

where the subscript means the number of interface.

The first order fields are solved by balancing the first order terms of Equations (10)–(12).

The matrix form is

$$\bar{\bar{Z}}^{(1)}\bar{U}^{(1)} = \bar{R}^{(1)} \tag{C4}$$

where $\bar{\bar{Z}}^{(1)}$ is a $(2n+2)\times(2n+2)$ matrix, and $\bar{U}^{(1)}$ is a $(2n+2)\times 1$ unknown vector.

$\bar{R}^{(1)}$ is the product of zeroth order solutions and first order scattering potentials

$$\bar{R}^{(1)} = -\bar{\bar{V}}_c^{(1)}\bar{\bar{U}}_D^{(0)}\bar{F} \tag{C5}$$

where $\bar{\bar{V}}_c^{(1)}$ is the $(2n+2)\times(2n+2)$ first order potential matrix, $\bar{\bar{U}}_D^{(0)}$ is the $(2n+2)\times(2n+2)$ diagonal matrix of zeroth order solution, and $\bar{F}$ is an aligned $(2n+2)\times 1$ vector composed of Fourier transforms of interfaces. However, there is no need to generate the surface profiles $\bar{F}$ while only $\bar{\bar{V}}_c^{(1)}$ and $\bar{\bar{U}}_D^{(0)}$ are necessary.

The first order surface fields can be found expressed as

$$\bar{U}^{(1)} = \left[\begin{array}{cccccccc} A_0^{(1)}(k_x,k_{ix}) & B_0^{(1)}(k_x,k_{ix}) & \cdots & A_l^{(1)}(k_x,k_{ix}) & B_l^{(1)}(k_x,k_{ix}) & \cdots & A_n^{(1)}(k_x,k_{ix}) & B_n^{(1)}(k_x,k_{ix}) \end{array}\right]^T \tag{C6}$$

where each term is a summation of Fourier transforms weighted by Fourier coefficients.

The second order fields are solved by balancing the second order terms of Equations (10)–(12).

$$\bar{\bar{Z}}^{(2)}\bar{U}^{(2)} = \bar{R}^{(2)} \tag{C7}$$

Only the coherent averaging terms are needed to compute second order power.

$$< \bar{\bar{Z}}^{(2)} >< \bar{U}^{(2)} >=< \bar{R}^{(2)} > \tag{C8}$$

where $< \bar{\bar{Z}}^{(2)} >$ is coherent averaged second order impedance matrix, which equals to the zeroth order impedance matrix $\bar{\bar{Z}}^{(0)}$ because of the delta function $\delta(k_x - k_{ix})$, $< \bar{U}^{(2)} >$ is the coherent average of the second order solutions.

The right hand side is composed of two parts: first is the product of zeroth order fields and second order scattering potentials, and second is the product of first order fields and first order scattering potentials.

Based on Equation (22) for uncorrelated relation of distinct rough interfaces, the right hand side can be separated into two parts:

$$< \bar{R}^{(2)} >=< \bar{R}_{02}^{(2)} > + < \bar{R}_{11}^{(2)} > \tag{C9}$$

where

$$< \bar{R}_{02}^{(2)} >= - < \bar{\bar{V}}_C^{(2)} > \bar{\bar{U}}_D^{(0)}\bar{W} \tag{C10}$$

where the $\bar{\bar{V}}_C^{(2)}$ is the $(2n+2)\times(2n+2)$ second order scattering potential matrix, and $\bar{\bar{U}}_D^{(0)}$ is the $(2n+2)\times(2n+2)$ diagonal matrix of zeroth order fields, $\bar{W}$ is the vector composed of $(2n+2)\times 1$ vector of spectral densities.

$$< \bar{R}_{11}^{(2)} >= - < \bar{\bar{V}}_C^{(1)} > \bar{\bar{I}} < \bar{\bar{U}}_D^{(1)} > \bar{W} \tag{C11}$$

where the $< \bar{\bar{V}}_C^{(1)} >$ is the $(2n+2)\times(2n+2)$ coherent averaged first order potential matrix, and $\bar{\bar{U}}_D^{(1)}$ is the $(2n+2)\times(2n+2)$ diagonal matrix of first order coefficients.

The second order surface fields can be expressed as

$$\begin{aligned} &< \bar{U}^{(2)} >= \\ &< [A_1^{(2)}(k_x,k_{ix})\ B_1^{(2)}(k_x,k_{ix}) \quad \ldots\ A_l^{(2)}(k_x,k_{ix})\ B_l^{(2)}(k_x,k_{ix}) \quad \ldots\ A_n^{(2)}(k_x,k_{ix})\ B_n^{(2)}(k_x,k_{ix})]^T > \end{aligned} \tag{C12}$$

where each term is a summation of spectral densities weighted by spectral density coefficients.

APPENDIX D. SCATTERED AND TRANSMITTED FIELDS AND POWERS

D.1. Scattered and Transmitted Fields

The scattering and transmission coefficients can be solved by applying the Green's theorem to the top and bottom regions.

The scattered wave is solved from

$$\psi_s\left(\bar{r}'\right) = \int_{S_0'} ds'\hat{n}_0' \cdot \left[\psi_0\left(\bar{r}'\right)\nabla g_0\left(\bar{r},\bar{r}'\right) - g_0\left(\bar{r},\bar{r}'\right)\nabla\psi_0\left(\bar{r}'\right)\right] \tag{D1}$$

by putting observation point in region 0.

The spectral domain solution of the scattered field is

$$\psi_s\left(k_x\right) = \frac{1}{2}A_0\left(k_x\right) + \int_{-\infty}^{\infty} dk_x' V_{00}^{N+}\left(k_x,k_x'\right) A_0\left(k_x'\right) - \frac{i}{2}\frac{1}{k_{0z}}B_0\left(k_x\right) - \int_{-\infty}^{\infty} dk_x' V_{00}^{D+}\left(k_x,k_x'\right) B_0\left(k_x'\right) \tag{D2}$$

Substituting the surface fields and scattering potentials, we obtain the zeroth, first, and coherent averaged second order scattered fields as follows

$$\tilde{\psi}_s^{(0)}\left(k_x\right) = \frac{1}{2}A_0^{(0)}\left(k_x\right) - \frac{i}{2}\frac{1}{k_{0z}}B_0^{(0)}\left(k_x\right) \tag{D3}$$

$$\psi_s^{(1)}\left(k_x\right) = \frac{1}{2}A_0^{(1)}\left(k_x\right) - \frac{i}{2}\frac{1}{k_{0z}}B_0^{(1)}\left(k_x\right) + V_{00}^{N+(1)}\left(k_x,k_x'\right) A_0^{(0)}\left(k_x'\right) - V_{00}^{D+(1)}\left(k_x,k_x'\right) B_0^{(0)}\left(k_x'\right) \tag{D4}$$

$$\begin{aligned} &< \psi_s^{(2)}(k_x) >= \frac{1}{2} < A_0^{(2)}(k_x) > - \frac{i}{2}\frac{1}{k_{0z}} < B_0^{(2)}(k_x) > + < V_{00}^{N+(2)}(k_x,k_{ix})A_0^{(0)}(k_{ix}) > \\ &- < V_{00}^{D+(2)}(k_x,k_{ix})B_0^{(0)}(k_{ix}) > + < V_{00}^{N+(1)}(k_x,k_x')A_0^{(1)}(k_x') > - < V_{00}^{D+(1)}(k_x,k_x')B_0^{(1)}(k_x') > \end{aligned} \tag{D5}$$

The first order scattered field is simplified as

$$\psi_s^{(1)}\left(k_x\right) = \sum_{l=0}^{n} \tilde{\psi}_{sl}^{(1)}\left(k_x,k_{ix}\right) F_l(k_x - k_{ix}) \tag{D6}$$

The coherent averaged second order scattered field is expressed as

$$< \psi_s^{(2)}(k_x) >= \delta(k_x - k_{ix}) \int_{-\infty}^{\infty} dk_x' \sum_{l=0}^{n} \tilde{\psi}_{sl}^{(2)}(k_x',k_{ix}) W_l(k_x' - k_{ix}) \tag{D7}$$

Similarly, the transmitted wave is solved from

$$\psi_t\left(\bar{r}'\right) = \int_{S_n'} ds\hat{n}_n' \cdot \left[\psi_n\left(\bar{r}'\right)\nabla g_{n+1}\left(\bar{r},\bar{r}'\right) - g_{n+1}\left(\bar{r},\bar{r}'\right)\nabla\psi_n\left(\bar{r}'\right)\right] \tag{D8}$$

by putting observation point in region $n+1$.

The spectral domain solution of the transmitted field is

$$\psi_t(k_x) = \frac{1}{2}e^{-ik_{(n+1)z}d_n}A_n(k_x) + \int_{-\infty}^{\infty} dk'_x V^{N-}_{n+1,n}\left(k_x,k'_x\right)A_n\left(k'_x\right) + \frac{i}{2}\frac{1}{k_{(n+1)z}}\frac{1}{\rho_{n,n+1}}e^{-ik_{(n+1)z}d_n}B_n(k_x) + \int_{-\infty}^{\infty} dk'_x V^{D-}_{n+1,n}\left(k_x,k'_x\right)B_n\left(k'_x\right) \tag{D9}$$

Substituting the surface fields and scattering potentials, we obtain the zeroth, first, and coherent averaged second order transmitted fields as follows

$$\tilde{\psi}^{(0)}_t(k_x) = \frac{1}{2}e^{-ik_{(n+1)z}d_n}A^{(0)}_n(k_x) + \frac{i}{2}\frac{1}{k_{(n+1)z}}\frac{1}{\rho_{n,n+1}}e^{-ik_{(n+1)z}d_n}B^{(0)}_n(k_x) \tag{D10}$$

$$\psi^{(1)}_t(k_x) = \frac{1}{2}e^{-ik_{(n+1)z}d_n}A^{(1)}_n(k_x) + \frac{i}{2}\frac{1}{k_{(n+1)z}}\frac{1}{\rho_{n,n+1}}e^{-ik_{(n+1)z}d_n}B^{(1)}_n(k_x) + V^{N-(1)}_{n+1,n}\left(k_x,k'_x\right)A^{(0)}_n\left(k'_x\right) + V^{D-(1)}_{n+1,n}\left(k_x,k'_x\right)B^{(0)}_n\left(k'_x\right) \tag{D11}$$

$$\begin{aligned}<\psi^{(2)}_t(k_x)> = {} & \frac{1}{2}e^{-ik_{(n+1)z}d_n}<A^{(2)}_n(k_x)> + \frac{i}{2}\frac{1}{k_{(n+1)z}}\frac{1}{\rho_{n,n+1}}e^{-ik_{(n+1)z}d_n}<B^{(2)}_n(k_x)> \\ & + <V^{N-(2)}_{n+1,n}(k_x,k'_x)A^{(0)}_n(k'_x)> + <V^{D-(2)}_{n+1,n}(k_x,k'_x)B^{(0)}_n(k'_x)> \\ & + <V^{N-(1)}_{n+1,n}(k_x,k'_x)A^{(1)}_n(k'_x)> + <V^{D-(1)}_{n+1,n}(k_x,k'_x)B^{(1)}_n(k'_x)>\end{aligned} \tag{D12}$$

The first order transmitted field is simplified as

$$\psi^{(1)}_t(k_x) = \sum_{l=0}^{n}\tilde{\psi}^{(1)}_{tl}(k_x,k_{ix})\,Fl(k_x-k_{ix}) \tag{D13}$$

The coherent averaged second order transmitted field is expressed as

$$<\psi^{(2)}_t(k_x)> = \delta(k_x-k_{tix})\int_{-\infty}^{\infty}dk'_x\sum_{l=0}^{n}\tilde{\psi}^{(2)}_{tl}\left(k'_x,k_{ix}\right)W_l(k'_x-k_{ix}) \tag{D14}$$

D.2. Scattered and Transmitted Powers per Unit Area

For TM polarization, the incident power is $<\bar{S}_{inc}\cdot(-\hat{z})>^{TM} = \frac{1}{2\omega\varepsilon_0}k_{0iz}$.

The scattered power can be divided into coherent and incoherent components:

$$\begin{aligned}<\bar{S}_s\cdot\hat{z}>^{TM}_{coh} = \mathrm{Re}\Bigg\{\frac{1}{2\omega\varepsilon_0}\Bigg[&<\psi^{(0)}_s(\bar{r})>\frac{\partial}{\partial z}<\psi^{(0)*}_s(\bar{r})> \\ &+<\psi^{(0)}_s(\bar{r})>\frac{\partial}{\partial z}<\psi^{(2)*}_s(\bar{r})> + <\psi^{(2)}_s(\bar{r})>\frac{\partial}{\partial z}<\psi^{(0)*}_s(\bar{r})>\Bigg]\Bigg\}\end{aligned} \tag{D15}$$

$$<\bar{S}_s\cdot\hat{z}>^{TM}_{incoh} = \mathrm{Re}\left\{\frac{1}{2\omega\varepsilon_0}\left[<\psi^{(1)}_s(\bar{r})>\frac{\partial}{\partial z}<\psi^{(1)*}_s(\bar{r})>\right]\right\} \tag{D16}$$

Substituting the spectral domain solution, we obtain

$$<\bar{S}_s\cdot\hat{z}>^{TM}_{coh} = \mathrm{Re}\left\{\frac{k_{0iz}}{2\omega\varepsilon_0}\left[\left|\tilde{\psi}^{(0)}_s(k_{ix})\right|^2 + 2\tilde{\psi}^{(0)}_s(k_{ix})\int_{-\infty}^{\infty}dk_x\sum_{l=0}^{n}\tilde{\psi}^{(2)}_{sl}(k_x,k_{ix})\,W_l(k_x-k_{ix})\right]\right\} \tag{D17}$$

$$<\bar{S}_s\cdot\hat{z}>^{TM}_{incoh} = \mathrm{Re}\left\{\frac{1}{2\omega\varepsilon_0}\left[\int_{-k_0}^{k_0}dk_x\sum_{l=0}^{n}k^*_z\left|\tilde{\psi}^{(1)}_{sl}(k_x,k_{ix})\right|^2 W_l(k_x-k_{ix})\right]\right\} \tag{D18}$$

Similarly, the transmitted power can be divided into coherent and incoherent components:

$$< \bar{S}_t \cdot (-\hat{z}) >_{coh}^{TM} = \mathrm{Re}\left\{ \frac{1}{2\omega\varepsilon_{n+1}} \left[< \psi_t^{(0)}(\bar{r}) > \frac{\partial}{\partial z} < \psi_t^{(0)*}(\bar{r}) > + < \psi_t^{(0)}(\bar{r}) > \frac{\partial}{\partial z} < \psi_t^{(2)*}(\bar{r}) > \right.\right.$$
$$\left.\left. + < \psi_t^{(2)}(\bar{r}) > \frac{\partial}{\partial z} < \psi_t^{(0)*}(\bar{r}) > \right] \right\} \tag{D19}$$

$$< \bar{S}_t \cdot (-\hat{z}) >_{incoh}^{TM} = \mathrm{Re}\left\{ \frac{1}{2\omega\varepsilon_{n+1}} \left[< \psi_t^{(1)}(\bar{r}) > \frac{\partial}{\partial z} < \psi_t^{(1)*}(\bar{r}) > \right] \right\} \tag{D20}$$

Substituting the spectral domain solution, we obtain

$$< \bar{S}_t \cdot (-\hat{z}) >_{coh}^{TM} = \mathrm{Re}\left\{ \frac{k_{(n+1)iz}}{2\omega\varepsilon_{n+1}} \left[\left| \tilde{\psi}_t^{(0)}(k_{ix}) \right|^2 + 2\tilde{\psi}_t^{(0)}(k_{ix}) \int_{-\infty}^{\infty} dk_x \sum_{l=0}^{n} \tilde{\psi}_{tl}^{(2)}(k_x, k_{ix}) W_l(k_x - k_{ix}) \right] \right\} \tag{D21}$$

$$< \bar{S}_t \cdot (-\hat{z}) >_{incoh}^{TM} = \mathrm{Re}\left\{ \frac{1}{2\omega\varepsilon_{n+1}} \left[\int_{-k_{n+1}}^{k_{n+1}} dk_x \sum_{l=0}^{n} k_{(n+1)z}^{*} \left| \tilde{\psi}_{tl}^{(1)}(k_x, k_{ix}) \right|^2 W_l(k_x - k_{ix}) \right] \right\} \tag{D22}$$

We examine the second order kernel functions (normalized by the incident power) as follows

$$\begin{aligned}
r_{coh}^{TM(2)} &= 2\mathrm{Re}\left[\tilde{\psi}_s^{(0)}(k_{ix}) \int_{-\infty}^{\infty} dk_x \sum_{l=0}^{n} \tilde{\psi}_{sl}^{(2)}(k_x, k_{ix}) W_l(k_x - k_{ix}) \right] \\
t_{coh}^{TM(2)} &= 2\mathrm{Re}\left\{ \frac{\varepsilon_0}{\varepsilon_{n+1}} \frac{k_{(n+1)iz}}{k_{0iz}} \left[\tilde{\psi}_t^{(0)}(k_{ix}) \int_{-\infty}^{\infty} dk_x \sum_{l=0}^{n} \tilde{\psi}_{tl}^{(2)}(k_x, k_{ix}) W_l(k_x - k_{ix}) \right] \right\} \\
r_{incoh}^{TM(2)} &= \mathrm{Re}\left\{ \frac{1}{k_{0iz}} \left[\int_{-k_0}^{k_0} dk_x \sum_{l=0}^{n} k_{0z}^{*} \left| \tilde{\psi}_{sl}^{(1)}(k_x, k_{ix}) \right|^2 W_l(k_x - k_{ix}) \right] \right\} \\
t_{incoh}^{TM(2)} &= \mathrm{Re}\left\{ \frac{\varepsilon_0}{\varepsilon_{n+1}} \frac{1}{k_{0iz}} \left[\int_{-k_{n+1}}^{k_{n+1}} dk_x \sum_{l=0}^{n} k_{(n+1)z}^{*} \left| \tilde{\psi}_{tl}^{(1)}(k_x, k_{ix}) \right|^2 W_l(k_x - k_{ix}) \right] \right\}
\end{aligned} \tag{D23}$$

It is noted that the incoherent waves arise only from the propagating waves, where for scattered wave $k_x \in [-k_0, k_0]$ and for transmitted wave $k_x \in [-k_{n+1}, k_{n+1}]$. The coherent waves are from both the propagating waves and the evanescent waves where $k_x \in [-\infty, \infty]$.

For TE polarization, the incident power is $< \bar{S}_{inc} \cdot (-\hat{z}) >^{TE} = \frac{1}{2\omega\mu_0} k_{0iz}$.

Using same procedure, we obtain

$$\begin{aligned}
r_{coh}^{TE(2)} &= 2\mathrm{Re}\left[\tilde{\psi}_s^{(0)}(k_{ix}) \int_{-\infty}^{\infty} dk_x \sum_{l=0}^{n} \tilde{\psi}_{sl}^{(2)}(k_x, k_{ix}) W_l(k_x - k_{ix}) \right] \\
t_{coh}^{TE(2)} &= 2\mathrm{Re}\left\{ \frac{\mu_0}{\mu_{n+1}} \frac{k_{(n+1)iz}}{k_{0iz}} \left[\tilde{\psi}_t^{(0)}(k_{ix}) \int_{-\infty}^{\infty} dk_x \sum_{l=0}^{n} \tilde{\psi}_{tl}^{(2)}(k_x, k_{ix}) W_l(k_x - k_{ix}) \right] \right\} \\
r_{incoh}^{TE(2)} &= \mathrm{Re}\left\{ \frac{1}{k_{0iz}} \left[\int_{-k_0}^{k_0} dk_x \sum_{l=0}^{n} k_{0z}^{*} \left| \tilde{\psi}_{sl}^{(1)}(k_x, k_{ix}) \right|^2 W_l(k_x - k_{ix}) \right] \right\} \\
t_{incoh}^{TE(2)} &= \mathrm{Re}\left\{ \frac{\mu_0}{\mu_{n+1}} \frac{1}{k_{0iz}} \left[\int_{-k_{n+1}}^{k_{n+1}} dk_x \sum_{l=0}^{n} k_{(n+1)z}^{*} \left| \tilde{\psi}_{tl}^{(1)}(k_x, k_{ix}) \right|^2 W_l(k_x - k_{ix}) \right] \right\}
\end{aligned} \tag{D24}$$

REFERENCES

1. Tsang, L., J. A. Kong, and K. H. Ding, *Scattering of Electromagnetic Waves, Vol. 1: Theory and Applications*, 426 pages, Wiley Interscience, 2000.

2. Tsang, L. and J. A. Kong, *Scattering of Electromagnetic Waves, Vol. 3: Advanced Topics*, 413 pages, Wiley Interscience, 2001.
3. Tsang, L., X. Gu, and H. Braunisch, "Effects of random rough surface on absorption by conductors at microwave frequencies," *IEEE Microwave and Wireless Components Letters*, Vol. 16, No. 4, 221–223, 2006.
4. Bagley, J. Q., L. Tsang, K. H. Ding, and A. Ishimaru, "Optical transmission through a plasmon film lens with small roughness: Enhanced spatial resolution of images of single source and multiple sources," *Journal of the Optical Society of America B*, Vol. 28, No. 7, 1766–1777, 2011.
5. Tsang, L., K. H. Ding, X. Li, P. N. Duvelle, J. H. Vella, J. Goldsmith, C. L. H. Devlin, and N. I. Limberopoulos, "Studies of the influence of deep subwavelength surface roughness on fields of plasmonic thin film based on Lippmann-Schwinger equation in the spectral domain," *Journal of the Optical Society of America B*, Vol. 32, No. 5, 878–891, 2015.
6. Tabatabaeenejad, A. and M. Moghaddam, "Bistatic scattering from three-dimensional layered rough surfaces," *IEEE Transactions on Geoscience and Remote Sensing*, Vol. 44, No. 8, 2102–2114, 2006.
7. Afifi, S. and R. Dusseaux, "On the co-polarized scattered intensity ratio of rough layered surfaces: The probability law derived from the small perturbation method," *IEEE Transactions on Antennas Propagation*, Vol. 60, No. 4, 2133–2138, 2012.
8. Johnson, J. T., "Third-order small-perturbation method for scattering from dielectric rough surfaces," *Journal of the Optical Society of America A*, Vol. 16, No. 11, 2720–2736, 1999.
9. Chiu, T. C. and K. Sarabandi, "Electromagnetic scattering interaction between a dielectric cylinder and a slightly rough surface," *IEEE Transaction on Antennas and Propagation*, Vol. 47, No. 5, 902–913, 1999.
10. Soubret A., G. Berginc, and C. Bourrely, "Backscattering enhancement of an electromagnetic wave scattered by two-dimensional rough layers," *Journal of the Optical Society of America A*, Vol. 18, No. 11, 2778–2788, 2001.
11. Demir, M. A. and J. T. Johnson, "Fourth and higher-order small perturbation solution for scattering from dielectric rough surfaces," *Journal of the Optical Society of America A*, Vol. 20, No. 12, 2330–2337, 2003.
12. Soubert A., G. Berginc, and C. Bourrely, "Application of reduced Rayleigh equations to electromagnetic wave scattering by two-dimensional randomly rough surfaces," *Physical Review B*, Vol. 63, No. 24, 245411, 2011.
13. Zamani, H., A. Tavakoli, and M. Dehmollaian, "Second-order perturbative solution of scattering from two rough surfaces with arbitrary dielectric profiles," *IEEE Transactions on Antennas and Propagation*, Vol. 63, No. 12, 5767–5776, 2015.
14. Zamani, H., A. Tavakoli, and M. Dehmollaian, "Second-order perturbative solution of cross-polarized scattering from multilayered rough surfaces," *IEEE Transactions on Antennas and Propagation*, Vol. 64, No. 5, 1877–1890, 2016.
15. Demir, M. A., "Perturbation theory of electromagnetic scattering from layered media with rough interfaces," Ph.D. Dissertation, Department of Electrical and Computer Engineering, The Ohio State University, Columbus, OH, 2007.
16. Imperatore, P., A. Iodice, and D. Riccio, "Electromagnetic wave scattering from layered structures with an arbitrary number of rough interfaces," *IEEE Transactions on Geoscience and Remote Sensing*, Vol. 47, No. 4, 1056–1072, 2009.
17. Wu, C. and X. Zhang, "Second-order perturbative solutions for 3-D electromagnetic radiation and propagation in a layered structure with multilayer rough interfaces," *IEEE Journal of Selected Topics in Applied Earth Observations and Remote Sensing*, Vol. 8, No. 1, 180–194, 2015.
18. Zamani, H., A. Tavakoli, and M. Dehmollaian, "Scattering from layered rough surfaces: Analytical and numerical investigations," *IEEE Transactions on Geoscience and Remote Sensing*, Vol. 54, No. 6, 3685–3696, 2016.
19. Demir, M. A., J. T. Johnson, and T. J. Zajdel, "A study of the fourth-order small perturbation method for scattering from two-layer rough surfaces," *IEEE Transactions on Geoscience and*

Remote Sensing, Vol. 50, No. 9, 3374–3382, 2012.

20. Pinel, N., J. T. Johnson, and C. Bourlier, "A geometrical optics model of three dimensional scattering from a rough layer with two rough surfaces," *IEEE Transactions on Antennas and Propagation*, Vol. 58, No. 3, 809–816, 2010.
21. Tabatabaeenejad, A., X. Duan, and M. Moghaddam, "Coherent scattering of electromagnetic waves from two-layer rough surfaces within the Kirchhoff regime," *IEEE Transactions on Geoscience and Remote Sensing*, Vol. 51, No. 7, 3943–3953, 2013.
22. Huang, S. and L. Tsang, "Electromagnetic scattering of randomly rough soil surfaces based on numerical solutions of Maxwell equations in three-dimensional simulations using a hybrid UV/PBTG/SMCG method," *IEEE Transactions on Geoscience and Remote Sensing*, Vol. 50, No. 10, 4025–4035, 2012.
23. Chen, K. S., T. D. Wu, L. Tsang, Q. Li, J. Shi, and A. K. Fung, "Emission of rough surfaces calculated by the integral equation method with comparison to three-dimensional moment method simulations," *IEEE Transactions on Geoscience and Remote Sensing*, Vol. 41, No. 1, 90–101, 2003.
24. Du, Y., J. A. Kong, Z. Y. Wang, W. Z. Yan, and L. Peng, "A statistical integral equation model for shadow-corrected EM scattering from a Gaussian rough surface," *IEEE Transactions on Antennas and Propagation*, Vol. 55, No. 6, 1843–1855, 2007.
25. Kuo, C. H. and M. Moghaddam, "Scattering from multilayer rough surfaces based on the extended boundary condition method and truncated singular value decomposition," *IEEE Transactions on Antennas and Propagation*, Vol. 54, No. 10, 2917–2929, 2006.
26. Kuo, C. H. and M. Moghaddam, "Electromagnetic scattering from multilayer rough surfaces with arbitrary dielectric profiles for remote sensing of subsurface soil moisture," *IEEE Transactions on Geoscience and Remote Sensing*, Vol. 45, No. 2, 349–366, 2007.
27. Duan, X. and M. Moghaddam, "3-D vector electromagnetic scattering from arbitrary random rough surfaces using stabilized extended boundary condition method for remote sensing of soil moisture," *IEEE Transactions on Geoscience and Remote Sensing*, Vol. 50, No. 1, 87–103, 2011.
28. Duan, X. and M. Moghaddam, "Bistatic vector 3-D scattering from layered rough surfaces using stabilized extended boundary condition method," *IEEE Transactions on Geoscience and Remote Sensing*, Vol. 51, No. 5, 2722–2733, 2013.
29. Jezek, K. C., J. T. Johnson, M. R. Drinkwater, G. Macelloni, L. Tsang, M. Aksoy, and M. Durand, "Radiometric approach for estimating relative changes in intraglacier average temperature," *IEEE Transactions on Geoscience and Remote Sensing*, Vol. 53, No. 1, 134–143, 2015.
30. Tan, S., M. Aksoy, M. Brogioni, G. Macelloni, M. Durand, K. C. Jezek, T. L. Wang, L. Tsang, J. T. Johnson, M. R. Drinkwater, and L. Brucker, "Physical models of layered polar firn brightness temperatures from 0.5 to 2 GHz," *IEEE Journal of Selected Topics in Applied Earth Observations and Remote Sensing*, Vol. 8, No. 7, 3681–3691, 2015.
31. Brogioni, M., G. Macelloni, F.Montomoli, and K. C.Jezek, "Simulating multifrequency ground-based radiometric measurements at Dome C-Antarctica," *IEEE Journal of Selected Topics in Applied Earth Observations and Remote Sensing*, Vol. 8, No. 9, 4405–4417, 2015.
32. Tsang, L., J. A. Kong, K. H. Ding, and C. O. Ao, *Scattering of Electromagnetic Waves, Vol. 2: Numerical Simulations*, 705 pages, Wiley Interscience, 2001.
33. Johnson, J. T. and M. Zhang, "Theoretical study of the small slope approximation for ocean polarimetric thermal emission," *IEEE Transactions on Geoscience and Remote Sensing*, Vol. 37, No. 5, 2305–2316, 1999.